Available online at www.sciencedirect.com
SCIENCE DIRECT®
Computers and Structures 82 (2004) 1131–1141
Computers & Structures
www.elsevier.com/locate/compstruc

A state space finite element for laminated composites with free edges and subjected to transverse and in-plane loads

J.Q. Ye [a,*], H.Y. Sheng [b], Q.H. Qin [c]

[a] School of Civil Engineering, University of Leeds, Leeds, LS2 9JT, UK
[b] Department of Building Engineering, Hefei University of Technology, Hefei, China
[c] School of Aerospace, Mechanical and Mechatronic Engineering, University of Sydney, Sydney, NSW 2006, Australia

Received 2 June 2003; accepted 18 March 2004
Available online 30 April 2004

Abstract

On the basis of the theory of three-dimensional elasticity, this paper presents a state space finite element solution for the stresses in cross-ply laminates subjected to combined transverse and in-plane loads. The state space formulation is introduced to solve for through-thickness stress distributions, while the traditional finite elements are used to approximate in-plane variations of the state variables. One of the direct applications of this solution is for the analysis of free-edge effect in cross-ply laminates. By appropriately describing the applied in-plane boundary tractions or boundary displacements, plates having complete free edges or boundary cross-sections with localized stress-free surfaces can be analyzed. Compared with the traditional finite element method, the new solution provides not only continuous through-thickness distributions of both displacements and transverse stresses, but also excellent approximations to the stress singularities in the vicinity of free edges or the above-mentioned localized stress-free surfaces.

Keywords: Free edge; Laminate; Ply crack; Stress concentration; Stress transfer

1. Introduction

The rapid increase of the industrial use of structures made of advanced composite materials, e.g. laminated materials, has necessitated the development of new numerical tools which are suitable for the analysis and study of mechanical behavior of such structures. It has been recognized that the prediction of their behavior, including the behavior of material interfaces, should be based on a three-dimensional rather than the conventional two-dimensional approaches. However, most existing mathematical models of multi-laminated materials have serious limitations and are incapable of giving satisfactory predictions over full ranges of performance of the materials.

Conventional finite element analyses are based on a representation for displacement field that guarantees the continuity of all displacement components across the element boundaries. The stress field derived from the displacement representation by use of the stress–strain relations leads to a stress field that is usually discontinuous across element boundaries. For many problems mesh refinement or element enhancement (see, for example, [1,17]) can minimize such discontinuities and lead to more accurate predictions for the stress field. The problem may also be dealt with using a two-dimensional layer-wise mixed theory [4–6] that is based on the application of Reissner's variational principle [19,20] to laminated structures. The theory uses both displacements and transverse stresses as primary variables at a layer level, where the number of unknown variables in the final linear algebra equations depends on the number of layers. An extensive review of the work published in this area can be found in [7]. These analyses aim at

* Corresponding author. Fax: +44-0113-2332265.
E-mail address: j.ye@leeds.ac.uk (J.Q. Ye).

0045-7949/$ - see front matter
doi:10.1016/j.compstruc.2004.03.020

assessing their numerical performance in predicting through-thickness stresses on cross-sections where stress concentration or singularities do not present. By using both displacements and transverse stresses as primary variables, Fan and Ye [10] proposed a three-dimensional state space method for analytical analysis of laminated plates. The state space method, which was also called the method of initial functions [23] or the transfer matrix method [3], takes the primary variables as state variables, the values of which at a particular through-thickness location, e.g., at bottom surface of a laminated plate, can uniquely define the state of the plate at any other through-thickness locations. Detailed description of the method can be found from [8,26]. A state space finite element method was further proposed by Sheng and Ye [21,22]. Once again these analyses concentrated solely on assessing numerical performance of the method for plates without stress singularities.

There are problems, however, that lead to stress field singularities where the traditional finite element analysis predictions of the stress field near such singularities are highly inaccurate. One example of such singularities occurs at stress-free edges of layered materials. The singularity occurs also at the boundary between two layers that have different material properties. Other types of singularity occur, for example, at the tips of ply cracks in composite laminates. In order to develop improved methods of analysis that can be applied to layered materials in structures subjected to complex loadings, it is essential that the new types of methods are capable of providing continuous fields of both interface tractions and displacements at the interfaces between layers. For simple loading and boundary conditions, analytical solutions have been obtained to approximate the singularities. For examples, a solution on the basis of the higher order plate theory was obtained by Becker [2]. By using the theory of two-dimensional elasticity, McCartney [13] proposed a generalized plane strain approach for some regular systems, such as flat plate layered systems and axisymmetric layered systems (see also, [14–16]). The model can ensure the continuity of both interface tractions and displacements. The approach can be thought of as being equivalent to a finite super-element where the elements are plates that are bonded together in the through-thickness direction. The through-thickness variations of stresses and displacements are modeled by layer refinement, while the in-plane variations are modeled by solutions of fourth order ordinary differential equations.

In this paper, a state space finite element method that combines the traditional finite element approximation and the recursive formulation of state space equation [10,26] is proposed to solve the stress problems of laminated plates subjected to combinations of transverse loads and in-plane boundary tractions and, especially, the stress problems with the above-mentioned singularities. The method is based on an early version of the method that has been used successfully for laminated plates without considering in-plane loading and stress singularities [21,22]. The state space method was also used by Wang et al. [24] to solve problems involving stress singularities, where an analytical solution based on eigen-expansion method was obtained for laminated rectangular strips. The current method is based on a mixed variational principle that includes the variations of both displacements and transverse stresses. By using the method, a plate is divided into finite elements in the plane of the plate, while the through-thickness distributions of the displacements and stresses are solved directly from the state space equation. Because of the applied boundary tractions, the resulting state space equation is non-homogeneous that is different to the one presented in [21,22]. To solve the new state equation, a new numerical procedure is proposed for the solution of the non-homogeneous state equation. Apart from the new theoretical and numerical development, this paper also aims at assessing the effectiveness of using the state space finite element for problems with material discontinuities and stress singularities. To this end, numerical examples are presented to validate the solution and comparisons are made between the new results and those obtained using alternative approaches.

2. The principles of variation and finite element approximations

Consider herewith a thick plate of uniform thickness h. The two in-plane co-ordinate parameters and the transverse co-ordinate are denoted, respectively, by x, y and z, while u, v and w represent the associated displacement components. The plate is subjected to a combination of transverse loads and in-plane boundary tractions. It is assumed that the plate is made of N different orthotropic material layers, each of which may have different thickness. For simplicity and convenience,

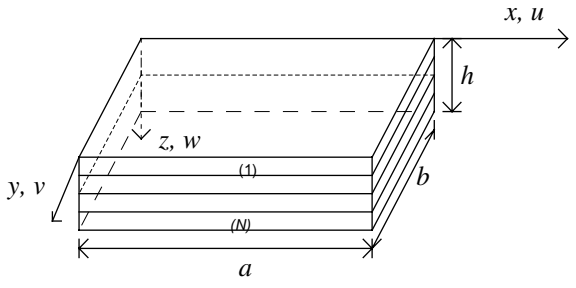

Fig. 1. Nomenclature of a laminated rectangular plate.

it is further assumed that the material axes of the orthotropic layers coincide with the axes of the adopted rectangular co-ordinate system. The geometry and co-ordinate system are shown in Fig. 1 for a rectangular plate, though the deduction and calculations shown in subsequent sections are not restricted to rectangular boundaries.

On the basis of the well-known Hellinger–Reissner variational principle [12,18,25], the following variational equation can be established for a material layer:

$$\int\int\int_V \delta\boldsymbol{\sigma}^{\mathrm{T}}[\mathbf{E}(\nabla)\mathbf{u}-\boldsymbol{\varepsilon}]\,\mathrm{d}V-\int\int\int_V \delta\mathbf{u}^{\mathrm{T}}[\mathbf{E}(\nabla)\boldsymbol{\sigma}+\mathbf{f}]\,\mathrm{d}V-\int\int_{B_u}\delta\mathbf{p}^{\mathrm{T}}(\mathbf{u}-\bar{\mathbf{u}})\,\mathrm{d}S+\int\int_{B_\sigma}\delta\mathbf{u}^{\mathrm{T}}(\mathbf{p}_s-\bar{\mathbf{p}}_s)\,\mathrm{d}S=0 \tag{1}$$

where variations are taken for both stresses and displacements. The definitions of the displacement and stress vectors and the differential operators, $\mathbf{E}(\nabla)$, can be found from [22]. In the above equation, B_u and B_σ denote displacement and stress boundaries, respectively. $\bar{\mathbf{u}}$ and $\bar{\mathbf{p}}_s$ are the respective displacements and tractions prescribed on the boundaries. The stresses and strains satisfy the Hooke's law of orthotropic materials that has also been defined in [22].

Assuming that the stress and displacement fields satisfy all prescribed boundary conditions, the following variational equation system can be used as an equivalent form of Eq. (1):

$$\int\int\int_V \delta\mathbf{u}^{\mathrm{T}}[\mathbf{E}(\nabla)\boldsymbol{\sigma}+\mathbf{f}]\,\mathrm{d}V=0 \tag{2}$$

$$\int\int\int_V \delta\boldsymbol{\sigma}^{\mathrm{T}}[\boldsymbol{\varepsilon}-\mathbf{E}^{\mathrm{T}}(\nabla)\mathbf{u}]\,\mathrm{d}V=0 \tag{3}$$

where the equilibrium equations of stresses and the strain-displacement relations are satisfied in the form of Galerkin weighting.

The stress analysis in the following sections uses both Eqs. (2) and (3) simultaneously, which forms a mixed representation of the variational principle and provides the theoretical foundation of the present method.

In order to solve the stress problem, the traditional finite element method is used first to approximate the in-plane variations of displacements and stresses. In this paper, this is achieved by introducing an iso-parametric element that has the traditional finite element features in the x–y plane, while the node parameters are taken as functions of the z-co-ordinate. Thus, the displacement and stress fields for a typical element, e.g., the kth element, of the laminated plate are described as follows:

$$\begin{aligned}
u^k &= \sum_{i=1}^{n} N_i^k(\xi,\eta)u_i^k(z)\\
v^k &= \sum_{i=1}^{n} N_i^k(\xi,\eta)v_i^k(z)\\
w^k &= \sum_{i=1}^{n} N_i^k(\xi,\eta)w_i^k(z)\\
\sigma_{xz}^k &= \sum_{i=1}^{n} N_i^k(\xi,\eta)\sigma_{xz_i}^k(z)\\
\sigma_{yz}^k &= \sum_{i=1}^{n} N_i^k(\xi,\eta)\sigma_{yz_i}^k(z)\\
\sigma_{xy}^k &= \sum_{i=1}^{n} N_i^k(\xi,\eta)\sigma_{xy_i}^k(z)\\
\sigma_{xx}^k &= \sum_{i=1}^{n} N_i^k(\xi,\eta)\sigma_{xx_i}^k(z)\\
\sigma_{yy}^k &= \sum_{i=1}^{n} N_i^k(\xi,\eta)\sigma_{yy_i}^k(z)\\
\sigma_{zz}^k &= \sum_{i=1}^{n} N_i^k(\xi,\eta)\sigma_{zz_i}^k(z)
\end{aligned} \tag{4}$$

In Eq. (4), ξ and η are local co-ordinates; $N_i^k(\xi,\eta)$ are shape functions and n denotes total node number of the element. $u_i^k(z)$, $\sigma_{xz_i}^k(z)$, etc., are functions of z and hence are named either node displacement or node stress function. It is worth mentioning that the three in-plane stresses are used initially as primary variables in the finite element analysis. This is necessary for the introduction of boundary tractions along edges of a plate. The in-plane stresses at any interior locations, however, will subsequently be eliminated from the formulation. Thus, the final linear algebra equation system will not include in-plane stresses as primary variables.

3. State space equation for a material layer

Substitute Eq. (4) into Eqs. (2) and (3) and consider all elements of the layer yield the following two variational equations that are presented in terms of the above-mentioned node functions. In the equations, the body forces, $\mathbf{f}$, are ignored.

$$\int_z \begin{Bmatrix}\delta\mathbf{p}\\ \delta\mathbf{q}\end{Bmatrix}^{\mathrm{T}}\left([\mathbf{A}]\frac{\mathrm{d}}{\mathrm{d}z}\begin{Bmatrix}\mathbf{p}\\ \mathbf{q}\end{Bmatrix}-[\mathbf{B}]\begin{Bmatrix}\mathbf{p}\\ \mathbf{q}\end{Bmatrix}+[\mathbf{C}]\{\mathbf{S}\}\right)\mathrm{d}z=0 \tag{5}$$

$$\int_z \{\delta\mathbf{S}\}^{\mathrm{T}}\left([\mathbf{D}]\{\mathbf{S}\}-[\mathbf{E}]\begin{Bmatrix}\mathbf{p}\\ \mathbf{q}\end{Bmatrix}\right)\mathrm{d}z=0 \tag{6}$$

where $\{\mathbf{p}\}^{\mathrm{T}}=[\mathbf{u}(z),\mathbf{v}(z),\mathbf{w}(z)]$, $\{\mathbf{q}\}^{\mathrm{T}}=[\boldsymbol{\sigma}_{xz}(z),\boldsymbol{\sigma}_{yz}(z),\boldsymbol{\sigma}_{zz}(z)]$ and $\{\mathbf{S}\}^{\mathrm{T}}=[\boldsymbol{\sigma}_{xx}(z),\boldsymbol{\sigma}_{yy}(z),\boldsymbol{\sigma}_{xy}(z)]$. These are vectors composed of the node functions shown in Eq. (4).

The node functions in the vectors are arranged in ascending order of node number, e.g. $\mathbf{u}(z) = [u_1(z), u_2(z), \ldots, u_M(z)]$, where M is the total node number of the plate. The constant matrices in Eqs. (5) and (6) can be calculated from Eq. (12c) in [22]. Eqs. (5) and (6) include variations of both displacements and stresses and are called mixed variational equations.

On the basis of the principle of variation, it is evident that Eqs. (5) and (6) are equivalent to the following equation system:

$$[\mathbf{A}]\frac{\mathrm{d}}{\mathrm{d}z}\begin{Bmatrix}\mathbf{p}\\ \mathbf{q}\end{Bmatrix} - [\mathbf{B}]\begin{Bmatrix}\mathbf{p}\\ \mathbf{q}\end{Bmatrix} + [\mathbf{C}]\{\mathbf{S}\} = 0 \tag{7}$$

$$[\mathbf{D}]\{\mathbf{S}\} - [\mathbf{E}]\begin{Bmatrix}\mathbf{p}\\ \mathbf{q}\end{Bmatrix} = \mathbf{0} \tag{8}$$

To facilitate the introduction of boundary conditions, the node function vectors in Eqs. (7) and (8) may be partitioned into two parts as shown below,

$$\{\mathbf{p}\} = \begin{Bmatrix}\mathbf{p}_f\\ \mathbf{p}_o\end{Bmatrix}, \quad \{\mathbf{q}\} = \begin{Bmatrix}\mathbf{q}_f\\ \mathbf{q}_o\end{Bmatrix}, \quad \{\mathbf{S}\} = \begin{Bmatrix}\mathbf{S}_f\\ \mathbf{S}_o\end{Bmatrix} \tag{9}$$

where $\mathbf{p}_f$, $\mathbf{q}_f$ and $\mathbf{S}_f$ consist of all unknown node functions while $\mathbf{p}_o$, $\mathbf{q}_o$ and $\mathbf{S}_o$ are the boundary node functions that have been prescribed by either given stresses or given displacements, i.e.

$$\{\mathbf{p}_o\} = \{\bar{\mathbf{p}}\}, \quad \{\mathbf{q}_o\} = \{\bar{\mathbf{q}}\}, \quad \{\mathbf{S}_o\} = \{\bar{\mathbf{S}}\} \tag{10}$$

The variation of Eq. (9) yields

$$\{\delta\mathbf{p}\} = \begin{Bmatrix}\delta\mathbf{p}_f\\ 0\end{Bmatrix}, \quad \{\delta\mathbf{q}\} = \begin{Bmatrix}\delta\mathbf{q}_f\\ 0\end{Bmatrix}$$
$$\{\delta\mathbf{S}\} = \begin{Bmatrix}\delta\mathbf{S}_f\\ 0\end{Bmatrix} \tag{11}$$

Accordingly, Eqs. (5) and (6) can be written as

$$\int_Z \begin{Bmatrix}\delta\mathbf{p}_f\\ 0\\ \delta\mathbf{q}_f\\ 0\end{Bmatrix}^{\mathrm{T}} \left([\mathbf{A}]\frac{\mathrm{d}}{\mathrm{d}z}\begin{Bmatrix}\mathbf{p}_f\\ \bar{\mathbf{p}}\\ \mathbf{q}_f\\ \bar{\mathbf{q}}\end{Bmatrix} - [\mathbf{B}]\begin{Bmatrix}\mathbf{p}_f\\ \bar{\mathbf{p}}\\ \mathbf{q}_f\\ \bar{\mathbf{q}}\end{Bmatrix} + [\mathbf{C}]\begin{Bmatrix}\mathbf{S}_f\\ \bar{\mathbf{S}}\end{Bmatrix} \right) \mathrm{d}z = 0 \tag{12}$$

$$\int_Z \begin{Bmatrix}\delta\mathbf{S}_f\\ 0\end{Bmatrix}^{\mathrm{T}} \left([\mathbf{D}]\begin{Bmatrix}\mathbf{S}_f\\ \bar{\mathbf{S}}\end{Bmatrix} - [\mathbf{E}]\begin{Bmatrix}\mathbf{p}_f\\ \bar{\mathbf{p}}\\ \mathbf{q}_f\\ \bar{\mathbf{q}}\end{Bmatrix} \right) \mathrm{d}z = 0 \tag{13}$$

that can be reduced to the following form:

$$\int_Z \{\delta\mathbf{R}\}^{\mathrm{T}} \Big([\mathbf{A}_f]\frac{\mathrm{d}}{\mathrm{d}z}\{\mathbf{R}\} - [\mathbf{B}_f]\{\mathbf{R}\} + [\mathbf{C}_f]\{\mathbf{S}_f\} - \{\mathbf{a}_f\} \Big) \mathrm{d}z = 0 \tag{14}$$

$$\int_Z \{\delta\mathbf{S}_f\}^{\mathrm{T}} \big([\mathbf{D}_f]\{\mathbf{S}_f\} - [\mathbf{E}_f]\{\mathbf{R}\} - \{\mathbf{b}_f\} \big) \mathrm{d}z = 0 \tag{15}$$

where $\{\mathbf{R}\} = \begin{bmatrix}\mathbf{p}_f^{\mathrm{T}} & \mathbf{q}_f^{\mathrm{T}}\end{bmatrix}^{\mathrm{T}}$; $\{\mathbf{a}_f\}$ and $\{\mathbf{b}_f\}$ are known vectors whose elements are related to $\{\bar{\mathbf{p}}\}$, $\{\bar{\mathbf{q}}\}$ and $\{\bar{\mathbf{S}}\}$. If $\{\bar{\mathbf{p}}\}$, $\{\bar{\mathbf{q}}\}$ and $\{\bar{\mathbf{S}}\}$ are all zero, $\{\mathbf{a}_f\}$ and $\{\mathbf{b}_f\}$ vanish from Eqs. (14) and (15).

Due to the variation of $\delta\mathbf{R}_f$ and $\delta\mathbf{S}_f$, Eqs. (14) and (15) are equivalent to

$$[\mathbf{A}_f]\frac{\mathrm{d}}{\mathrm{d}z}\{\mathbf{R}\} = [\mathbf{B}_f]\{\mathbf{R}\} - [\mathbf{C}_f]\{\mathbf{S}_f\} + \{\mathbf{a}_f\} \tag{16}$$

$$[\mathbf{D}_f]\{\mathbf{S}_f\} = [\mathbf{E}_f]\{\mathbf{R}\} + \{\mathbf{b}_f\} \tag{17}$$

The in-plane stress vector $\{\mathbf{S}_f\}$ discontinues across contact layers in general. Eliminating $\{\mathbf{S}_f\}$ from Eqs. (15) and (16) the vector yields

$$\frac{\mathrm{d}}{\mathrm{d}z}\{\mathbf{R}\} = [\mathbf{T}]\{\mathbf{R}\} + \{\mathbf{B}\} \tag{18}$$

where

$$[\mathbf{T}] = [\mathbf{A}_f]^{-1}\Big([\mathbf{B}_f] - [\mathbf{C}_f][\mathbf{D}_f]^{-1}[\mathbf{E}_f] \Big)$$
$$\{\mathbf{B}\} = [\mathbf{A}_f]^{-1}\Big(\{\mathbf{a}_f\} - [\mathbf{C}_f][\mathbf{D}_f]^{-1}\{\mathbf{b}_f\} \Big) \tag{19}$$

Eq. (18) is known as non-homogeneous state equation that can be solved either numerically or analytically. For problems of small degrees of freedom, an analytical expression of the solution can be obtained. Otherwise, an approximate solution has to be sought [26].

In general, for a N-plied laminate composed of orthotropic layers, the state space equation for an arbitrary layer, e.g., the jth ($j = 1, 2, \ldots, N$) layer, can always be expressed as

$$\frac{\mathrm{d}}{\mathrm{d}z}\{\mathbf{R}_j(z)\} = [\mathbf{T}_j]\{\mathbf{R}_j(z)\} + \{\mathbf{B}_j(z)\}, \quad 0 \leqslant z \leqslant h_j \tag{20}$$

4. Solutions of non-homogeneous state equations

In this section, a new and efficient numerical procedure is introduced to solve Eq. (20). Consider first the case where the jth material layer of the laminate is sufficiently thin such that $\{\mathbf{R}_j(z)\}$ and $\{\mathbf{B}_j(z)\}$ can be, respectively, approximated by $(\{\mathbf{R}_j(h_j)\} + \{\mathbf{R}_j(0)\})/2$ and $(\{\mathbf{B}_j(h_j)\} + \{\mathbf{B}_j(0)\})/2$. Thus, Eq. (20) is calculated as follows:

$$\int_0^{h_j} \mathrm{d}\{\mathbf{R}_j\} = \int_0^{h_j} [\mathbf{T}_j]\{\mathbf{R}_j\}\mathrm{d}z + \int_0^{h_j} \{\mathbf{B}_j\}\mathrm{d}z \tag{21}$$

Because $[\mathbf{T}_j]$ is a constant matrix, the above equation yields

$$\{\mathbf{R}_j(h_j)\} - \{\mathbf{R}_j(0)\} = \frac{h_j}{2}[\mathbf{T}_j](\{\mathbf{R}_j(h_j)\} + \{\mathbf{R}_j(0)\}) + \frac{h_j}{2}(\{\mathbf{B}_j(h_j)\} + \{\mathbf{B}_j(0)\}) \tag{22}$$

Introducing

$$[\mathbf{A}] = \frac{h_j}{2}[\mathbf{T}_j]$$

$$\{\mathbf{B}_j^*\} = \frac{h_j}{2}(\{\mathbf{B}_j(h_j)\} + \{\mathbf{B}_j(0)\})$$

into Eq. (22) yields

$$(\mathbf{I} - \mathbf{A})\{\mathbf{R}_j(h_j)\} = (\mathbf{I} + \mathbf{A})\{\mathbf{R}_j(0)\} + \{\mathbf{B}_j^*\} \tag{23}$$

In the case where the jth material layer is not sufficiently thin, we can divide the layer into K_j sub-layers of equal thickness Δ_j, each of which is sufficiently thin. Hence, for the first sub-layer of the jth material layer, for example, we have

$$\int_0^{\Delta_j} \mathrm{d}\{\mathbf{R}_j\} = \int_0^{\Delta_j} [\mathbf{T}_j]\{\mathbf{R}_j\}\mathrm{d}z + \int_0^{\Delta_j} \{\mathbf{B}_j\}\mathrm{d}z \tag{24}$$

Applying the same assumption as the one used to obtain Eqs. (22) and (23) yields

$$(\mathbf{I} - \mathbf{A})\{\mathbf{R}_j^{(1)}(\Delta_j)\} = (\mathbf{I} + \mathbf{A})\{\mathbf{R}_j^{(1)}(0)\} + \{\mathbf{B}_j^{(1)}\} \tag{25}$$

where

$$[\mathbf{A}] = \frac{\Delta_j}{2}[\mathbf{T}_j]$$

$$\{\mathbf{B}_j^{(1)}\} = \frac{\Delta_j}{2}(\{\mathbf{B}_j(\Delta_j)\} + \{\mathbf{B}_j(0)\})$$

In general, for the ith sub-layer of the jth material layer, we have

$$(\mathbf{I} - \mathbf{A})\{\mathbf{R}_j^{(i)}(i\Delta_j)\} = (\mathbf{I} + \mathbf{A})\{\mathbf{R}_j^{(i-1)}((i-1)\Delta_j)\} + \{\mathbf{B}_j^{(i)}\} \tag{26}$$

where

$$\{\mathbf{B}_j^{(i)}\} = \frac{\Delta_j}{2}(\{\mathbf{B}_j(i\Delta_j)\} + \{\mathbf{B}_j((i-1)\Delta_j)\})$$

Starting with Eq. (25) and then using Eq. (26) and the following continuity condition:

$$\{\mathbf{R}_j^{(i)}(0)\} = \{\mathbf{R}_j^{(i-1)}((i-1)\Delta_j)\} \tag{27}$$

we obtain for the jth material layer

$$(\mathbf{I} - \mathbf{A})^{K_j}\{\mathbf{R}_j(h_j)\} = (\mathbf{I} + \mathbf{A})^{K_j}\{\mathbf{R}_j(0)\} + \sum_{i=1}^{K_j}(\mathbf{I} + \mathbf{A})^{K_j - i}(\mathbf{I} - \mathbf{A})^{i-1}\{\mathbf{B}_j^{(i)}\} \tag{28}$$

It is worthwhile to mention that the identity shown below is used in the deduction process of Eq. (28):

$$(\mathbf{I} - \mathbf{A})(\mathbf{I} + \mathbf{A}) = (\mathbf{I} + \mathbf{A})(\mathbf{I} - \mathbf{A}) \tag{29}$$

The matrices, $(\mathbf{I} - \mathbf{A})^{K_j}$ and $(\mathbf{I} + \mathbf{A})^{K_j}$, can be calculated efficiently by using the iteration process proposed by Zhong and Williams [27], where K_j is chosen as power of 2, i.e., $K_j = 2^k$.

Solving Eq. (28) results in

$$\{\mathbf{R}_j(h_j)\} = [\mathbf{Z}_j(h_j)]\{\mathbf{R}_j(0)\} + \{\mathbf{H}_j\} \tag{30}$$

for the jth material layer. After finding the solutions in the form of Eq. (30) for all material layers of the laminate, the final equation for the entire laminate can be obtained by imposing the continuity conditions

$$\{\mathbf{R}_j(h_j)\} = \{\mathbf{R}_{j+1}(0)\} \tag{31}$$

at all material interfaces and recursively using Eqs. (30) and (31), as follows:

$$\begin{aligned}\{\mathbf{R}_N(h_N)\} &= [\mathbf{Z}_N(h_N)]\{\mathbf{R}_N(0)\} + \{\mathbf{H}_N\} \\ &= [\mathbf{Z}_N(h_N)]([\mathbf{Z}_{N-1}(h_{N-1})]\{\mathbf{R}_{N-1}(0)\} \\ &\quad + \{\mathbf{H}_{N-1}\}) + \{\mathbf{H}_N\} \\ &= \cdots = [\mathbf{D}]\{\mathbf{R}_1(0)\} + \{\mathbf{\Pi}\}\end{aligned} \tag{32}$$

where

$$[\mathbf{D}] = \prod_{k=N}^{1}[\mathbf{Z}_k(h_k)]$$

$$\{\mathbf{\Pi}\} = \left(\prod_{k=N}^{2}[\mathbf{Z}_k(h_k)]\right)\{\mathbf{H}_1\} + \left(\prod_{k=N}^{3}[\mathbf{Z}_k(h_k)]\right)\{\mathbf{H}_2\} + \cdots + [\mathbf{Z}_N(h_N)]\{\mathbf{H}_{N-1}\} + \{\mathbf{H}_N\}$$

In Eq. (32), $\{\mathbf{R}_N(h_N)\}$ and $\{\mathbf{R}_1(0)\}$ are the node function vectors consisting of displacements and transverse stresses on the bottom ($z = h$) and top ($z = 0$) surfaces of the laminate, respectively. By introducing load conditions (tractions) on the two plate surfaces into Eq. (32), a set of linear algebra equations in terms of the node displacement functions are formed, from which the solution of the problem can be obtained. It is worth mentioning that the order of Eq. (32) is identical to that of Eq. (30). Hence, it is a fact that the order of Eq. (32) depends solely on the finite element meshes used in the x–y plane and is completely independent of the number of material layers of the composite plate.

In the case of a uniformly distributed pressure, $\boldsymbol{\omega}$, applied on the top surface of the laminated plate, for instance, the load conditions are

$$\begin{aligned}\{\mathbf{q}_f(0)\}_1^{\mathrm{T}} &= [\boldsymbol{\sigma}_{xz}(0), \boldsymbol{\sigma}_{yz}(0), \boldsymbol{\sigma}_{zz}(0)] = [\mathbf{0} \quad \mathbf{0} \quad -\boldsymbol{\omega}] \\ \{\mathbf{q}_f(h_N)\}_N^{\mathrm{T}} &= [\boldsymbol{\sigma}_{xz}(h), \boldsymbol{\sigma}_{yz}(h), \boldsymbol{\sigma}_{zz}(h)] = [\mathbf{0} \quad \mathbf{0} \quad \mathbf{0}]\end{aligned} \tag{33}$$

The subscripts, 1 and N, denote that the node function vectors are those of the top and bottom layers, respectively. Substituting Eq. (33) into Eq. (32), one yields the following linear algebra equation system:

$$\begin{bmatrix} \mathbf{D}_{41} & \mathbf{D}_{42} & \mathbf{D}_{43} \\ \mathbf{D}_{51} & \mathbf{D}_{52} & \mathbf{D}_{53} \\ \mathbf{D}_{61} & \mathbf{D}_{62} & \mathbf{D}_{63} \end{bmatrix} \begin{Bmatrix} \mathbf{u}_f(0) \\ \mathbf{v}_f(0) \\ \mathbf{w}_f(0) \end{Bmatrix}_1 = \left(\begin{bmatrix} \mathbf{D}_{46} \\ \mathbf{D}_{56} \\ \mathbf{D}_{66} \end{bmatrix} \{\boldsymbol{\omega}\} - \begin{Bmatrix} \boldsymbol{\Pi}_4 \\ \boldsymbol{\Pi}_5 \\ \boldsymbol{\Pi}_6 \end{Bmatrix} \right) \tag{34}$$

where the $\mathbf{D}_{ij}$, $\boldsymbol{\Pi}_i$ are the relevant sub-matrices of $[\mathbf{D}]$ and $\{\boldsymbol{\Pi}\}$ in Eq. (32), respectively, and $\{\boldsymbol{\omega}\}$ is the external load vector containing loads applied at the nodes on the top surface of the plate. Once the initial values of the node displacement functions, i.e. the values of node displacements at $z = 0$ are found, the displacements and stresses at any location throughout the thickness of the plate can be calculated by using Eq. (30).

5. Numerical examples

To validate the new method, numerical calculations are carried out first for a simply supported orthotropic square plate. The plate has the following material properties:

$$\begin{aligned} C_{12}/C_{11} &= 0.246269, \quad C_{13}/C_{11} = 0.0831715 \\ C_{22}/C_{11} &= 0.543103, \quad C_{23}/C_{11} = 0.115017 \\ C_{33}/C_{11} &= 0.530172, \quad C_{44}/C_{11} = 0.266810 \\ C_{55}/C_{11} &= 0.159914, \quad C_{66}/C_{11} = 0.262931 \end{aligned} \tag{35}$$

The plate is subjected to a uniformly distributed pressure, q, on the top surface and a pair of symmetrically applied in-plane pressure, q, along $x = 0$ and $x = a$. As a result of symmetry, only a quarter of the plate is analyzed in the following calculations. Eight-node quadrilateral elements are used in the x–y plane and the state equations are solved numerically by using the new technique described in Section 4. Since the convergence rate of the state space finite element method against finite element meshes has been tested in the previous work [22], the numerical validation presented here is only for assessing convergence against the number of sub-layers used in the solution of non-homogeneous state equations (see Section 4). Table 1 shows the following non-dimensional displacement and stress parameters for the plate with a thickness ratio $h/a = 0.8$, against the value of k that has been defined below Eq. (29).

$$\begin{aligned} \left(\bar{u} \quad \bar{v} \quad \bar{w}\right) &= \frac{C_{11}^{(c)}}{qh}\left(u \quad v \quad w\right) \\ \left(\bar{\sigma}_{xx} \quad \bar{\sigma}_{yy} \quad \bar{\sigma}_{xz} \quad \bar{\sigma}_{zz}\right) &= \left(\sigma_{xx} \quad \sigma_{yy} \quad \sigma_{xz} \quad \sigma_{zz}\right)/q \end{aligned} \tag{36}$$

It can be seen from Table 1 that the results converge rapidly. For displacements, a division of $\Delta_j/h \leqslant 0.1$ is sufficient for obtaining a satisfactory result. For stresses, further division is needed to achieve a result of the same accuracy. It can be concluded from Table 1 that the new procedure provides an effective and accurate tool for solving non-homogeneous state equations.

After testing the convergence of the new method, Table 2 shows stresses and displacements of a three-plied simply supported plate. The plate has two iden-

Table 1
Convergence rate against various values of k

	z/h	$h/a = 0.8$					
		$k = 3$	$k = 4$	$k = 5$	$k = 6$	$k = 7$	$k = 8$
$\bar{u}$	0.0	−0.24079	−0.24032	−0.24014	−0.24009	−0.24008	−0.24008
$x = 0$	0.5	−0.77801	−0.78239	−0.78190	−0.78178	−0.78175	−0.78174
$y = a/2$	1.0	−0.81899	−0.82372	−0.82447	−0.82465	−0.82470	−0.82471
$\bar{w}$	0.0	1.48886	1.49099	1.49151	1.49164	1.49168	1.49168
$x = a/2$	0.5	0.72290	0.72442	0.72481	0.72491	0.72493	0.72494
$y = a/2$	1.0	0.46244	0.46848	0.46996	0.47032	0.47043	0.47044
$\bar{\sigma}_{xx}$	0.0	0.08848	0.08625	0.08572	0.08559	0.08555	0.08555
$x = a/2$	0.5	1.09401	1.08836	1.08646	1.08601	1.08589	1.08589
$y = a/2$	1.0	1.45488	1.45933	1.46046	1.46074	1.46081	1.46082
$\bar{\sigma}_{xz}$	0.0	0.00000	0.00000	0.00000	0.00000	0.00000	0.00000
$x = 0$	0.5	0.32807	0.37801	0.37771	0.37761	0.37759	0.37758
$y = a/2$	1.0	0.00000	0.00000	0.00000	0.00000	0.00000	0.00000

Table 2
Stresses and displacements of three-plied laminated plates with various values of h/a ($\delta = 5$)

		$h/a = 0.4$		$h/a = 0.6$		$h/a = 0.8$	
		Present	Analytical	Present	Analytical	Present	Analytical
$\bar{u}$	T+	−0.79006	−0.79330	−0.63341	−0.63520	−0.48381	−0.48498
$x = 0$	T−	−1.47918	−1.48356	−1.10208	−1.10396	−0.85909	−0.86036
$y = a/2$	C+	−1.47918	−1.48356	−1.10208	−1.10396	−0.85909	−0.86036
	C−	−1.59105	−1.55045	−0.94785	−0.95049	−0.71160	−0.71364
	B+	−1.59105	−1.55045	−0.94785	−0.95049	−0.71160	−0.71364
	B−	−1.89379	−1.89729	−1.07723	−1.08006	−0.76234	−0.76458
$\bar{w}$	T+	3.74720	3.74918	1.74137	1.74335	1.15524	1.15620
$x = a/2$	T−	3.73358	3.73527	1.71581	1.71759	1.12581	1.12662
$y = a/2$	C+	3.73358	3.73527	1.71581	1.71759	1.12581	1.12662
	C−	2.92534	2.91861	0.84949	0.84701	0.29623	0.29516
	B+	2.92534	2.91861	0.84949	0.84701	0.29623	0.29516
	B−	2.89820	2.89164	0.83686	0.83452	0.28980	0.28887
$\bar{\sigma}_{xx}$	T+	1.43962	1.51988	2.92194	3.01145	3.07202	3.21483
$x = a/2$	T−	3.50041	3.68258	4.68769	4.82605	5.19854	5.40323
$y = a/2$	C+	0.58088	0.61626	0.81639	0.85493	0.91718	0.95712
	C−	1.30439	1.33912	1.03142	1.06813	0.97901	1.01654
	B+	6.55421	6.72872	5.19615	5.38059	4.93187	5.12054
	B−	8.70776	8.81822	6.72535	6.80513	5.93394	6.11717
$\bar{\sigma}_{yy}$	T+	−4.39704	−4.46059	−3.02735	−3.10024	−2.71629	−2.78970
$x = a/2$	T−	−3.02554	−3.07163	−1.85213	−1.88841	−1.34763	−1.37892
$y = a/2$	C+	−0.76995	−0.78063	−0.53796	−0.54678	−0.43897	−0.44661
	C−	0.26199	0.25201	−0.01383	−0.01305	−0.11669	−0.12554
	B+	1.35459	1.30588	−0.01514	−0.02001	−0.53248	−0.57535
	B−	2.77315	2.72534	0.95980	0.92332	0.06933	0.05524
$\bar{\sigma}_{zz}$	T+	−1.00000	−1.02562	−1.00000	−1.02562	−1.00000	−1.02562
$x = a/2$	T−	−0.94979	−0.95820	−0.96532	−0.97432	−0.97629	−0.98426
$y = a/2$	C+	−0.94979	−0.95820	−0.96532	−0.97432	−0.97629	−0.98426
	C−	−0.05144	−0.05280	−0.06222	−0.06366	−0.05873	−0.06032
	B+	−0.05144	−0.05280	−0.06222	−0.06366	−0.05873	−0.06032
	B−	0.00000	0.00000	0.00000	0.00000	0.00000	0.00000
$\bar{\sigma}_{xz}$	T+	0.00000	0.00000	0.00000	0.00000	0.00000	0.00000
$x = 0$	T−	1.10297	1.11176	0.86236	0.84445	0.75590	0.73002
$y = a/2$	C+	1.10297	1.11176	0.86236	0.84445	0.75590	0.73002
	C−	0.59315	0.61071	0.28813	0.31171	0.14342	0.16815
	B+	0.59315	0.61071	0.28813	0.31171	0.14342	0.16815
	B−	0.00000	0.00000	0.00000	0.00000	0.00000	0.00000

tical face layers and a core layer that have the same ratios of stiffness as shown in Eq. (36). The face and core layers are distinguished by the ratio $\delta = C_{11}^{(F)}/C_{11}^{(C)}$, where F and C denote face and core, respectively. The plate has a total thickness of h, of which the thickness of each face layer is $0.1h$. The plate is subjected to a uniformly distributed pressure, q, on the top surface and symmetric in-plane boundary pressures along $x = 0$ and $x = a$. The boundary pressures are layer-wise constant and are $5q$, q and $5q$, respectively, from the bottom layer. The results are calculated with $k = 8$ and compared with those obtained by a three-dimensional analytical solution in [9] that was based on using Fourier series expansion in the in-plane directions and analytical solution of differential equation in the transverse direction.

In Table 2, T denotes top layer, C denotes core layer and B denotes bottom layer. + and − indicate, respectively, top and bottom surfaces of a layer. From the results shown in the table, it is evident that the state space solution approaches the three-dimensional analytical one rapidly for both displacements and stresses. It can also been seen from the table that the numerical analysis provides continuous variations of both displacements and transverse stresses across all material interfaces.

To apply the state space finite element method to solve free edge problems, a four-layered cross-ply laminate ($[0/90]_s$) is considered. The following elastic constants are assumed:

$$C_{11} = C_{33} = 15300 \text{ N/mm}^2, \quad C_{22} = 140000 \text{ N/mm}^2$$
$$C_{44} = C_{55} = 5900 \text{ N/mm}^2, \quad C_{12} = C_{23} = 3900 \text{ N/mm}^2$$
$$C_{13} = 3300 \text{ N/mm}^2$$

The plate has two opposite free edges. The other two edges are subjected to a uniform strain ε_0.

In Figs. 2 and 3, the results obtained by using the state space finite element method are compared with those obtained by Becker [2] and Wang et al. [24] for interfacial shear and direct stresses, respectively, near the free edge at $x = 0$.

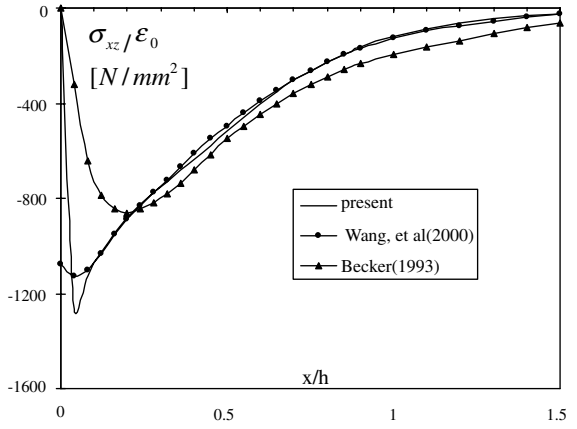

Fig. 2. Interfacial shear stress at the [0/90] interface.

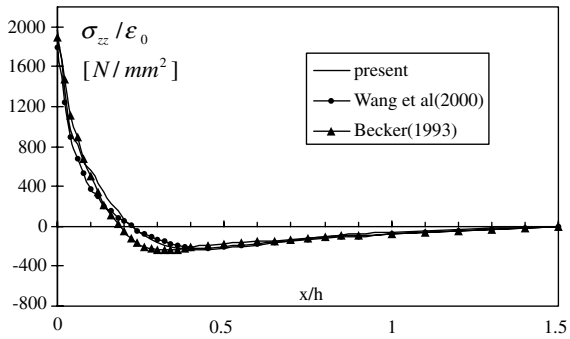

Fig. 3. Interfacial direct stress at the [0/90] interface.

Figs. 2 and 3 show high stress concentration near the free edge, and the stresses decay away rapidly towards the interior region of the laminate.

The second example of stress singularity is stresses in cross-ply laminates with uniformly distributed transverse ply cracks. Consider a composite laminate having a combination of 0° and 90° layers (Fig. 4a). It is assumed that the 90° ply has transverse cracks in the matrix that run through the entire width along the fiber direction. It is also assumed that the horizontal distribution of the cracks is equally spaced, so that a representative element (see Fig. 4b) in two neighboring cracks can be taken out and analyzed to minimize computing effort.

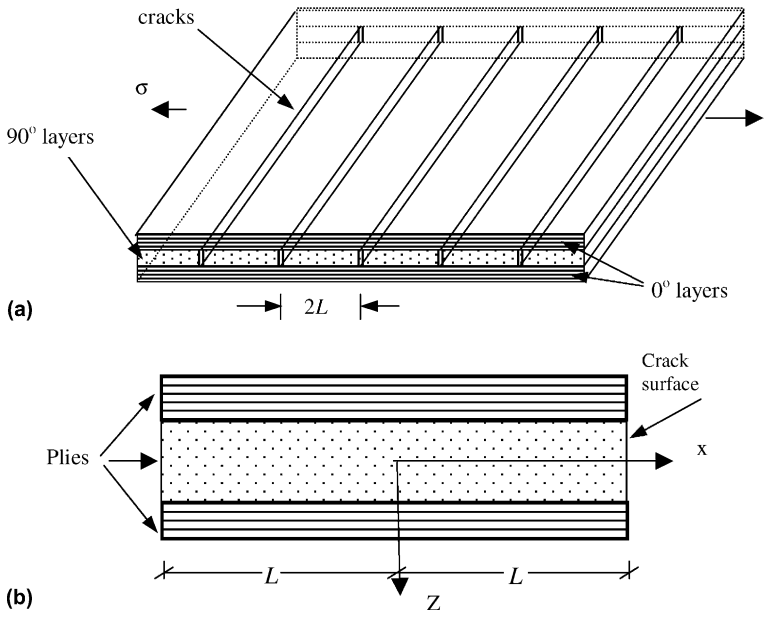

Fig. 4. (a) Cross-ply laminate with transverse cracks in 90° layer; (b) a representative element.

Assuming that the element is subjected to a linearly distributed strain, or a uniformly distributed strain when bending is absent, along the un-cracked surfaces at the two ends, the problem becomes a generalized plane strain problem. A two-dimensional analytical mode has been established by McCartney and Pierse [14] to calculate stress transfer in such a cracked laminate. As a part of validation of the present method, the interfacial shear and normal stresses at the interface between 0° ply and 90° ply of a four ply ($[0°/90°]_s$) graphite/epoxy laminate are calculated and compared with the results obtained using McCartney and Pierse's [14] solution. The laminate is subjected to a uni-axial average stress of $\sigma = 0.2$ GPa. The material properties used in the calculations for the graphite/epoxy laminates [11] are as follows:

$$E_L = 144.78 \text{ GPa}, \quad E_T = 9.58 \text{ GPa}$$
$$G_{LT} = 4.785 \text{ GPa}, \quad \nu_{LT} = 0.31, \quad \nu_{TT} = 0.55$$

The laminate has a crack separation space $2L = 4.0$ mm and an equal ply thickness $h_{ply} = 0.25$ mm.

In Figs. 5 and 6, the results obtained by using the state space finite element method and the two-dimensional plane strain model [14] are shown by the dotted lines and the solid lines, respectively. Excellent agreement is observed.

For through-thickness distributions of displacements and stresses, it has been shown from previous publications [21,22] that the results obtained from the state space finite element method agreed very well with existing three-dimensional analytical solutions, where stresses were calculated for plates without free edges or at locations away from free edges. In the following example, the transverse direct stress and the displacement in the x direction for the cracked laminate considered above are shown against the transverse co-ordinate at the location where stress singularity or material discontinuity occurs.

Fig. 7 presents the horizontal displacement at $x = L$ in the x direction of the representative element shown in Fig. 4b. Due to symmetry, only the distribution across top half of the element is plotted. In the figure, the state space finite element solution is denoted by the dots and the solution from the plane strain analytical model [14] is presented by the solid line. The displacement is virtually constant along the un-cracked surface ($-0.5 \leqslant z/h \leqslant -0.25$), while it is distributed non-linearly along the cracked surface ($-0.25 \leqslant z/h \leqslant 0$).

Fig. 8 shows the transverse direct stress at $x = L$ across the thickness of the element shown in Fig. 4b.

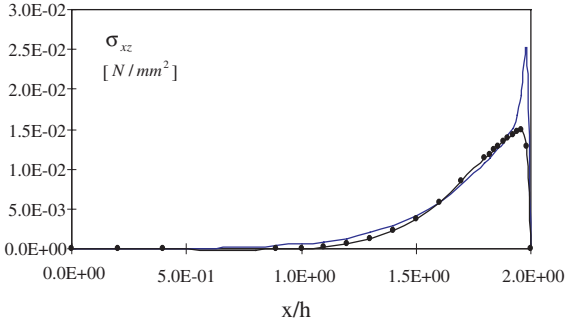

Fig. 5. Interfacial shear stress distribution at 0°/90° interface.

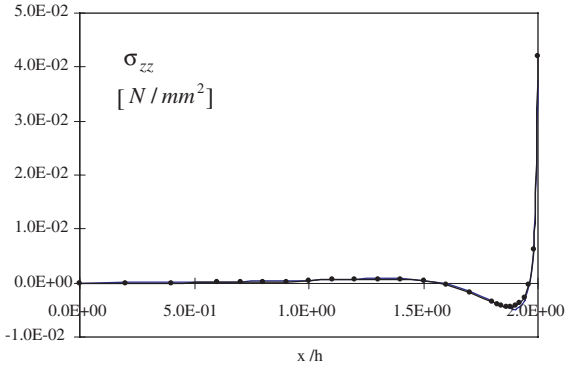

Fig. 6. Interfacial direct stress distribution at 0°/90° interface.

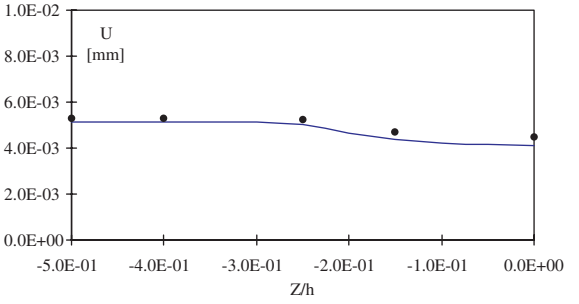

Fig. 7. Through-thickness horizontal displacement at $x = L$.

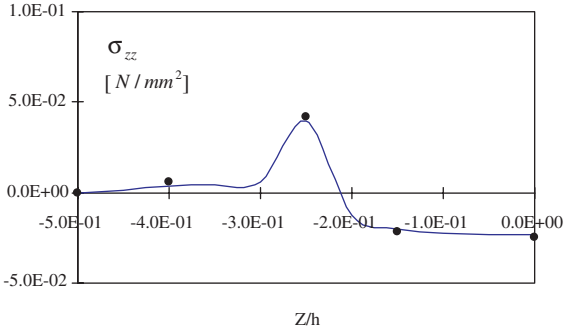

Fig. 8. Through-thickness distribution of transverse direct stress at $x = L$.

Once again the present results are compared with the ones based on the plane strain analytical model. It can be seen that stress concentration of the transverse direct stress near the crack tip ($z/h = -0.25$) is evident. The direct stress along the un-cracked surface is significantly smaller than that along the cracked surface.

6. Concluding remarks

A state space finite element method has been presented to solve three-dimensional stress problems of laminated plates subjected to combined transverse loads and in-plane boundary tractions. The applications of the method to the stress analysis of free edge effect were shown by numerical examples. The method was based on a mixed variational representation of the three-dimensional equations of elasticity. The in-plane fields of both displacements and stresses were approximated by finite elements while their through-thickness distributions were obtained by solving a system of non-homogeneous state equations.

A new numerical technique has been proposed to solve the non-homogeneous state equations. Numerical tests and comparisons have been carried out to validate the method. By comparing with existing three-dimensional analytical solutions, it was observed that the new method converged very fast and provided accurate results. It is worthwhile to mention that due to the use of the finite element approximation in the in-plane directions, the well-known singularities of interfacial shear stress that would have appeared at the interface near the free edges have been smoothed out. Numerical tests, which are not presented here, show that as more elements are used in the calculation, the peak shear stress increases and its location moves further towards the free edges. Thus, it is concluded that the proposed method can approximate the stress singularities near free edges or ply cracks of laminated composites.

Since the recursive formulation (see Eq. (31)) was used to derive the state equations of laminated plates, unlike most layer-wise based method, the dimension of the final linear algebra equation system did not depend on the number of material layers. This reduces the size of the final linear algebra equation system significantly and, hence, reduces the computer effort on solving the equation system. As a consequence, it can be concluded that this method is particularly suitable to solve stress problems of multi-layered composites.

The method always provides continuous distributions of both displacements and transverse stresses across perfectly bonded material boundaries. This reduces further the computer effort that has to be used in the traditional displacement-based finite element analyses to recover transverse stresses.

The method can be used to provide accurate numerical solutions that are useful for benchmark tests of new plate theories and finite element codes, especially when dealing with stress singularities or discontinuities. Since the present work aims at establishing the element and its numerical performance in dealing with free edges and cracks, the applications of the element to large complex structures are subjected to further investigation. However, due to the use of the standard finite element procedure in the proposed analysis, it is expected that it will be a straightforward extension to apply the method to, e.g., laminated plates with non-rectangular boundaries and plate assemblies, etc.

Acknowledgements

The first author is grateful for the financial support from the EPSRC, the Royal Academy of Engineering and the School of Aerospace, Mechanical and Mechatronic Engineering at the University of Sydney.

References

[1] Auricchio F, Sacco E. A mixed-enhanced Finite Element for the analysis of laminated composite plates. Int J Numer Meth Eng 1999;44:1481–504.
[2] Becker W. Closed-form solution for the free-edge effect in cross-ply laminates. Compos Struct 1993;26:39–45.
[3] Bufler H. Theory of elasticity of a multilayered medium. J Elasticity 1971;1:125–43.
[4] Carrera E. C_z^0 Reissner–Mindlin multilayered plate elements including zig-zag and interlaminar stress continuity. Int J Numer Eng 1996;39:1797–820.
[5] Carrera E. C_z^0-requirements: models for the two-dimensional analysis of multilayered structures. Compos Struct 1997;37:373–83.
[6] Carrera E. Evaluation of layerwise mixed theories form laminated plate analysis. AIAA J 1998;36(5):830–9.
[7] Carrera E. Developments, ideas and evaluation based upon Reissner's mixed variational theorem in the modeling of multilayered plates and shells. Appl Mech Rev 2001;54(4):301–29.
[8] DeRusso PM, Roy RJ, Close CM, Desrochers AA. State variables for engineers. John Wiley; 1998.
[9] Fan JR, Sheng HY. Exact solution for thick laminates acted by longitudinal and lateral loads. J Hefei University Technol 1992;15(1):10–9.
[10] Fan JR, Ye JQ. An exact solution for the statics and dynamics of laminated thick plates with orthotropic layers. Int J Solids Struct 1990;26(5/6):655–62.
[11] Groves SE, Harris CE, Highsmith AL, Allen DH, Norvell RG. An experimental and analytical treatment of matrix cracking in cross-ply laminates. Exp Mech 1987;27:73–9.
[12] Hu HC. Variational principles and their applications in mechanics of elasticity. Beijin: Science Press; 1981.

[13] McCartney LN. Theory of stress transfer in a 0°–90°–0° cross-ply laminate containing a parallel array of transverse cracks. J Mech Phys Solids 1992;40:27–69.
[14] McCartney LN, Pierse C. Stress transfer mechanics for multiple ply laminates subject to bending. NPL report CMMT(A) 55, 1997.
[15] McCartney LN, Pierse C. Stress transfer mechanics for multiple ply laminates for axial loading and bending. In: Proceedings of the 11th International Conference on Composite Materials, Gold Cost, Australia, July 14–18, 1997. p. 662–71.
[16] McCartney LN, Schoeppner GA, Becker W. Comparison of models for transverse ply cracks in composite laminates. Compos Sci Technol 2000;60:2347–59.
[17] Noor AK, Burton WS. Assessment of computational models for multi-layered composite shells. Appl Mech Rev 1990;43:67–97.
[18] Reissner E. On a variational theorem in elasticity. J Math Phys 1950;29:90–5.
[19] Reissner E. On a certain mixed variational theory and proposed applications. Int J Numer Eng 1984;20:1366–8.
[20] Reissner E. On a mixed variational theorem and on a shear deformable plate theory. Int J Numer Eng 1986;23:193–8.
[21] Sheng HY, Ye JQ. A semi-analytical finite element for laminated composite plates. Compos Struct 2002;57(1–4):117–23.
[22] Sheng HY, Ye JQ. A state space finite element for laminated composite plates. Comput Methods Appl Mech Eng 2002;191(37–38):4259–76.
[23] Vlasov VZ. The method of initial functions in problems of theory of thick plates and shells. In: Proc Ninth Int Congress Appl Mech, Brussels; 1957. p. 321–30.
[24] Wang YM, Tarn JQ, Hsu CK. State space approach for stress decay in laminates. Int J Solids Struct 2000;37:3535–53.
[25] Washizu K. Variational methods in elasticity and plasticity. 2nd ed. Pergamon Press; 1975.
[26] Ye JQ. Laminated composite plates and shells: 3D modelling. London: Springer-Verlag; 2002.
[27] Zhong WX, Williams FW. A precise time step integration method. Proc Inst Mech Eng 1994;208:427–30.